Human Molecular Genetics, 2018, Vol. 27, No. 11 1905–1912

doi: 10.1093/hmg/ddy097
Advance Access Publication Date: 15 March 2018
Original Article

ORIGINAL ARTICLE

Increased polyamines as protective disease modifiers in congenital muscular dystrophy

D.U. Kemaladewi[1], J.S. Benjamin[2,†], E. Hyatt[1], E.A. Ivakine[1] and R.D. Cohn[1,2,3,4,*]

[1]Program in Genetics and Genome Biology, The Hospital for Sick Children Research Institute, Toronto, ON M5G 0A4, Canada, [2]McKusick-Nathans Institute of Genetic Medicine, Johns Hopkins University School of Medicine, Baltimore, MD 21205, USA, [3]Department of Molecular Genetics, University of Toronto, Toronto, ON M5S 1A8, Canada and [4]Department of Pediatrics, University of Toronto, and The Hospital for Sick Children, Toronto, ON M5G 1X8, Canada

*To whom correspondence should be addressed. Tel: +1-416-813-6122; Fax: +1-416-813-7479; Email: ronald.cohn@sickkids.ca

Abstract

Most Mendelian disorders, including neuromuscular disorders, display extensive clinical heterogeneity that cannot be solely explained by primary genetic mutations. This phenotypic variability is largely attributed to the presence of disease modifiers, which can exacerbate or lessen the severity and progression of the disease. LAMA2-deficient congenital muscular dystrophy (LAMA2-CMD) is a fatal degenerative muscle disease resulting from mutations in the *LAMA2* gene encoding Laminin-α2. Progressive muscle weakness is predominantly observed in the lower limbs in LAMA2-CMD patients, whereas upper limbs muscles are significantly less affected. However, very little is known about the molecular mechanism underlying differential pathophysiology between specific muscle groups. Here, we demonstrate that the *triceps* muscles of the dy^{2j}/dy^{2j} mouse model of LAMA2-CMD demonstrate very mild myopathic findings compared with the *tibialis anterior* (TA) muscles that undergo severe atrophy and fibrosis, suggesting a protective mechanism in the upper limbs of these mice. Comparative gene expression analysis reveals that S-Adenosylmethionine decarboxylase (*Amd1*) and Spermine oxidase (*Smox*), two components of polyamine pathway metabolism, are downregulated in the TA but not in the triceps of dy^{2j}/dy^{2j} mice. As a consequence, the level of polyamine metabolites is significantly lower in the TA than triceps. Normalization of either *Amd1* or *Smox* expression in dy^{2j}/dy^{2j} TA ameliorates muscle fibrosis, reduces overactive profibrotic TGF-β pathway and leads to improved locomotion. In summary, we demonstrate that a deregulated polyamine metabolism is a characteristic feature of severely affected lower limb muscles in LAMA2-CMD. Targeted modulation of this pathway represents a novel therapeutic avenue for this devastating disease.

Introduction

Congenital muscular dystrophy (CMD) represents a highly heterogeneous group of disorders, manifesting as severe muscle wasting and poor motor movements, which appear at birth or shortly thereafter. Approximately 40% of CMD cases are classified as Laminin-α2 (previously called merosin)-deficient CMD (LAMA2-CMD), which is caused by mutations in the *LAMA2* gene. The Laminin-α2 is part of Laminin-211 protein complex, which is expressed in the basement membrane of muscle and Schwann cells (1–3). Consequently, children affected by LAMA2-CMD develop profound muscle hypotonia and weakness, accompanied by contractures or muscle tendons tightening,

[†]Present address: Department of Neurology, Building 100, Room B4-123 VAPAHCS 3801 Miranda Ave, Palo Alto, CA 94304, USA.
Received: October 10, 2017. **Revised:** February 8, 2018. **Accepted:** March 12, 2018

dysmyelinating neuropathy and white matter abnormalitites. Remarkably, the muscle-related phenotypes predominantly affect lower limbs, including hips, knees and ankles, which together contribute to their inability to walk (4–6). The clinical heterogeneity and variability in the extent of myopathy in different muscle groups led us to postulate a presence of disease-modifying factors in protected LAMA2-CMD muscles.

Similar to affected patients, the dy^{2j}/dy^{2j} mouse model of LAMA2-CMD exhibits an apparent hindlimb atrophy starting at 1 month of age (7), yet the forelimb muscles are only mildy affected. The dy^{2j}/dy^{2j} mouse model carries a splice-site mutation in the *Lama2* gene, causing exclusion of exon 2 from its transcript and production of a truncated, non-functional Lama2 protein (8,9). In our previous study, we have shown that CRISPR/Cas9-mediated correction of a splice-site mutation ameliorates the dystrophic phenotypes in the dy^{2j}/dy^{2j} mice (10). However, due to the heterogeneity of disease-causing mutations, translation of this strategy to patients is challenging.

This study is aimed at identifying disease-modifying factors underlying the myopathic heterogeneity between different muscle groups to develop a mutation-independent strategy to ameliorate dystrophic phenotypes in dy^{2j}/dy^{2j} mice. We performed comparative transcriptomic profiling and identified imbalanced polyamine metabolism as a contributing factor to previously unrecognized, distinctive myopathic phenotypes between *tibialis anterior* (TA) and *triceps*, which represent hind limb and forelimb muscles in dy^{2j}/dy^{2j} mice. We then developed a strategy to modulate polyamine level *in vivo* and observed improvement in dystrophic-associated fibrosis as well as locomotion.

Results

Severity of disease progression differ between hindlimb and forelimb muscles of dy^{2j}/dy^{2j} mice

We first determined whether significant phenotypic differences are present between hindlimb and forelimb muscles of the dy^{2j}/dy^{2j} mice at various stages of disease progression. TA and triceps from 3-, 5-, 12- and 20-week-old dy^{2j}/dy^{2j} mice were analyzed for the dystrophic pathophysiology. In agreement with previous reports, dy^{2j}/dy^{2j} mice become paralyzed at the age of 3 weeks and present with little to no mobility at the age of 20 weeks (7,11). In the TA muscles, we observed progressive inflammatory infiltration starting at 3 weeks onwards (Fig. 1a–d), with only sporadic presence of centrally nucleated fibers, suggestive of an inefficient regeneration process. The extent of fibrosis in the TA muscles increased over time, leading to augmented fibrotic tissue deposition at the age of 20 weeks old (Fig. 1d).

In contrast, severe inflammatory changes are observed in the triceps muscles starting from the early age of 3 weeks old, which recapitulates a previously reported study in dy^{W} mice demonstrating infiltration of mononucleated cells as an early signature of muscle pathology (7). However, the severe inflammation gradually decreases over time, with a nearly normal histology at the age of 20 weeks old (Fig. 1e–g). Centrally nucleated fibers are evident starting at the age of 5 weeks old onwards, and fibrosis is negligible in the triceps muscles compared with TA (Figs 1h and 2a). Analysis of muscle histology at the age of 12 weeks old showed ~5-fold less fibrotic tissue in the triceps compared with the TA (Fig. 2a). Truncated Lama2 protein is expressed at comparable level in TA and triceps (10) and thus cannot attribute to the stark phenotypic differences between the myopathy and regeneration capacity in both muscles. Taken together, our data suggest that an efficient regeneration process is likely responsible for the milder phenotype in the triceps.

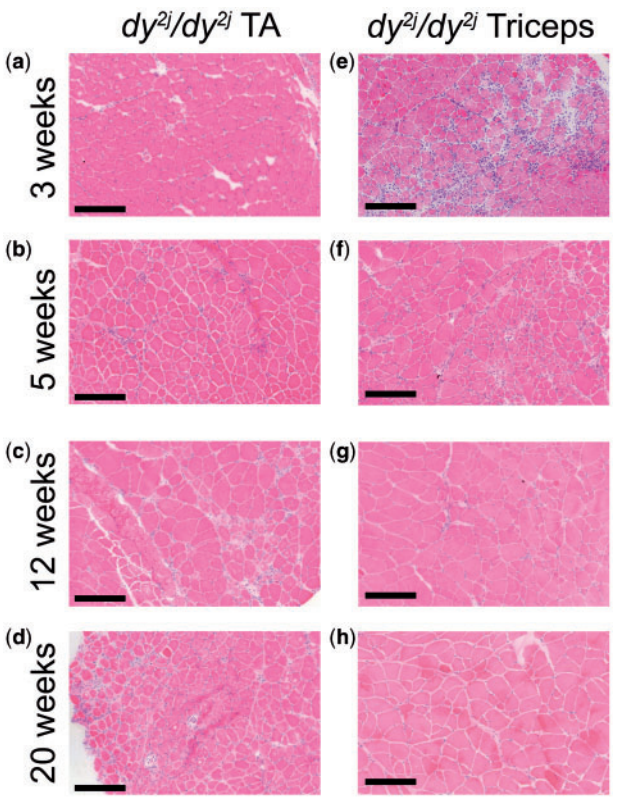

Figure 1. Distinctive histopathology between TA and triceps muscles in dy^{2j}/dy^{2j} mice during different stages of the disease. Cross-sections of TA and triceps muscles isolated from dy^{2j}/dy^{2j} mice at 3 weeks (**a, e**), 5 weeks (**b, f**), 12 weeks (**c, g**) and 20 weeks (**d, h**) were stained with H&E. Scale bars: 200 μm. Five animals were analyzed per age group, and figures are representative of 3–4 micrographs/animal.

Severe hindlimb myopathy in dy^{2j}/dy^{2j} mice is attributed to reduced expression of key enzymes in polyamine biogenesis pathway

To explore the pathogenetic mechanism underlying the discrepancies between hindlimb and forelimb muscle phenotypes, we compared global gene expression patterns in triceps and TA muscles of 12-week-old dy^{2j}/dy^{2j} mice using the Affymetrix 1.0 ST Gene Chip (Supplementary Material, Table S1). After excluding genes that were differentially expressed between TA and triceps in wild-type mice, we identified two genes that were significantly downregulated in dy^{2j}/dy^{2j} TA compared with dy^{2j}/dy^{2j} triceps, namely *Amd1* and *Smox* encoding S-Adenosylmethionine decarboxylase and Spermine oxidase, two key enzymes in polyamine biogenesis pathway (Supplementary Material, Table S2 and Fig. S1). Quantitative Real-Time PCR (qRT-PCR) confirmed that *Amd1* and *Smox* are expressed 15- and 8-fold lower in the TA muscles of dy^{2j}/dy^{2j} compared with triceps, respectively (Fig. 2b). There was no difference in the expression of *Amd1* and *Smox* between TA and triceps in wild-type mice, indicating that there is no intrinsic disparity between these muscle groups that could contribute to the imbalanced expression profiles in dy^{2j}/dy^{2j} mice (Fig. 2b).

We subsequently assessed Amd1 and Smox protein levels in dy^{2j}/dy^{2j} TA and triceps muscles at different ages across the disease progression, e.g. 1-, 3-, 12- and 20 weeks old (Fig. 2c and d,

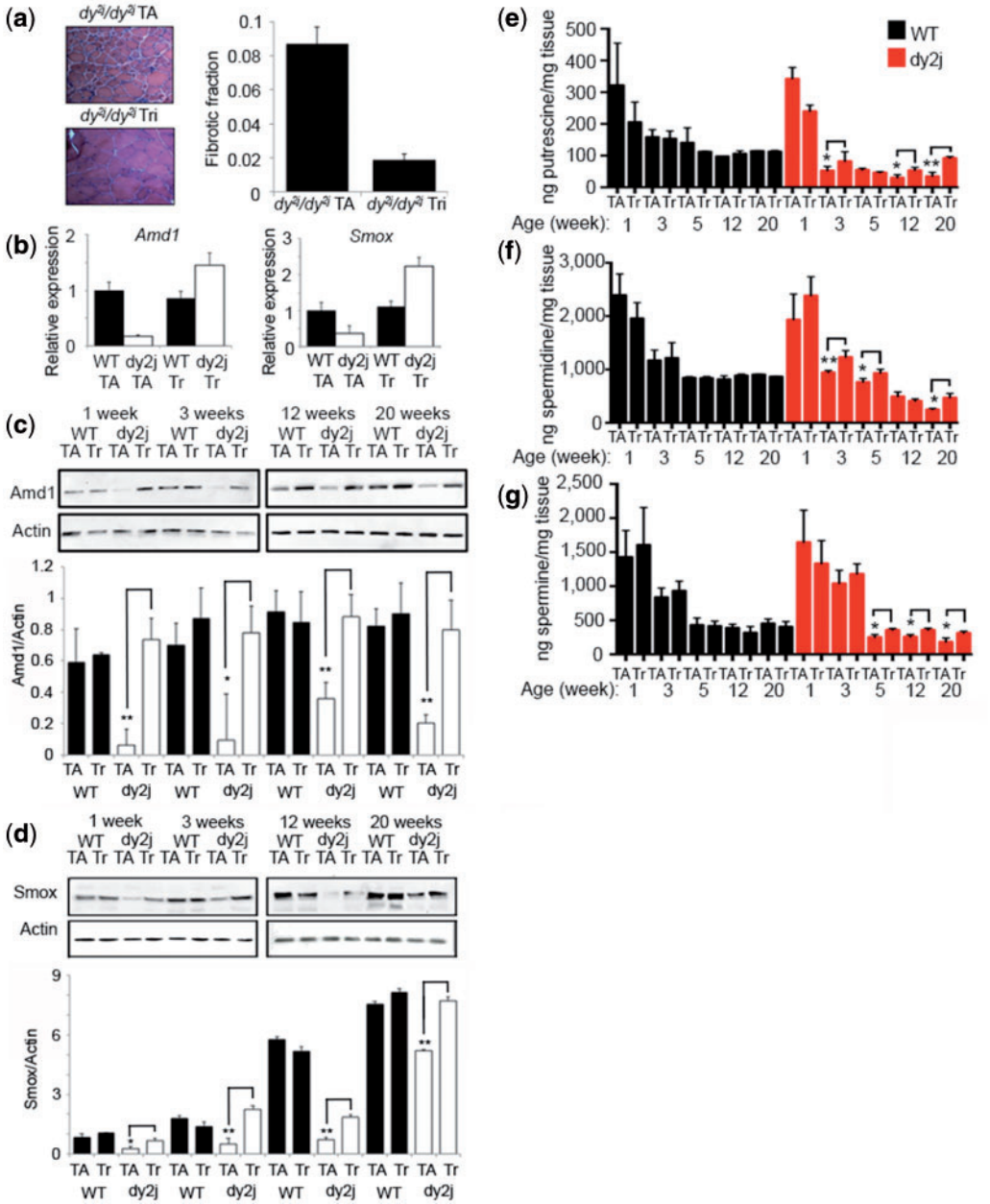

Figure 2. Imbalanced fibrosis, polyamine metabolizing enzymes and metabolite levels in TA and triceps of dy^{2j}/dy^{2j} mice. Quantification of fibrotic fraction in TA and triceps of 12-week-old dy^{2j}/dy^{2j} mice (**a**). Quantitative RT-PCR validation showing *Amd1* and *Smox* expression in TA and triceps of 12-week-old dy^{2j}/dy^{2j} and wild-type mice (**b**). Western blot and densitometry analyses showing Amd1 (**c**) and Smox (**d**) expression, normalized to Actin, in TA and triceps of wild-type and dy^{2j}/dy^{2j} mice at different ages. Quantification of putrescine (**e**), spermidine (**f**) and spermine (**g**) metabolites in TA and triceps from wild-type (black bars) and dy^{2j}/dy^{2j} (red bars) at 1-, 3-, 5-, 12- and 20 weeks old using LC-MS/MS. Error bars represent standard deviation from 4 to 5 animals/group. Statistical analysis was performed using Student's *t*-test. $^{*}P < 0.05$, $^{**}P < 0.01$.

Supplementary Material, Fig. S2). Both Amd1 (Fig. 2c) and Smox (Fig. 2d) are expressed at lower levels in TA compared with triceps continuously at all time points analyzed. These data suggest that reduced Amd1 and Smox protein levels may contribute to the disease severity phenotype in the dy^{2j}/dy^{2j} mice.

Decrease in Amd1 and Smox expression results in lower polyamine levels in severely affected TA muscles

Polyamines, small metabolites derived from L-arginine and methionine, are important for cell proliferation and their intracellular concentration is strictly regulated by a set of enzymes, including Amd1 and Smox. Decrease in the amount of polyamines interferes with cell growth (12), while excess appears to be toxic (13).

We investigated the consequences of low levels of Amd1 and Smox proteins by quantifying the amount of three most abundant polyamines: putrescine, spermidine and spermine using High performance liquid chromatography/mass spectrometry (HPLC-MS/MS) (Fig. 2e–g). We observed lower amounts of putrescine, spermidine and spermine in dy^{2j}/dy^{2j} TA compared with triceps, corroborating our observations of lower Amd1 and Smox protein levels in

TA muscles. Although slightly variable between the three polyamines and the age group analyzed, the differences were apparent starting at 3 weeks of age and became more evident at the later stage of the disease, reaching significance at 12 and 20 weeks.

Exogenous polyamine enhances dy^{2j}/dy^{2j} myoblast growth

Our comparative analysis suggests that, in contrast to the TA muscles, higher Amd1 and Smox expression in the triceps may contribute to its efficient regeneration process, and eventually the milder phenotypes. Therefore, to investigate whether modulation of polyamine is beneficial for cellular muscle growth under dystrophic condition, we isolated myoblasts from wild-type and dy^{2j}/dy^{2j} muscles and measured its proliferation rates (Fig. 3a, Supplementary Material, Fig. S3). Similar to previously reported findings, the dy^{2j}/dy^{2j} myoblasts proliferate slower than wild-type (7). Addition of 50 μM of putrescine into the culture media increased the dy^{2j}/dy^{2j} myoblast proliferation, whereas 500 nM of difluoromethylornithine (DFMO), an inhibitor of ornithine decarboxylase 1 (Odc1), a rate-limiting enzyme important for conversion of ornithine to putrescine (Supplementary Material, Fig. S1), inhibited the growth. Importantly, addition of putrescine was able to rescue the DFMO-mediated growth inhibition in dy^{2j}/dy^{2j} myoblasts.

Next, we asked whether overexpression of *Amd1* or *Smox* could enhance dy^{2j}/dy^{2j} myoblast growth. We found that either *Amd1* or *Smox* alone increased Ki67 expression, a marker for cell proliferation (Fig. 3b). However, we did not observe any synergistic effect on cell growth when both *Amd1* and *Smox* were overexpressed. Taken together, these data demonstrate the important role that polyamines play in muscle growth/homeostasis, which warrants further investigation of this pathway *in vivo*.

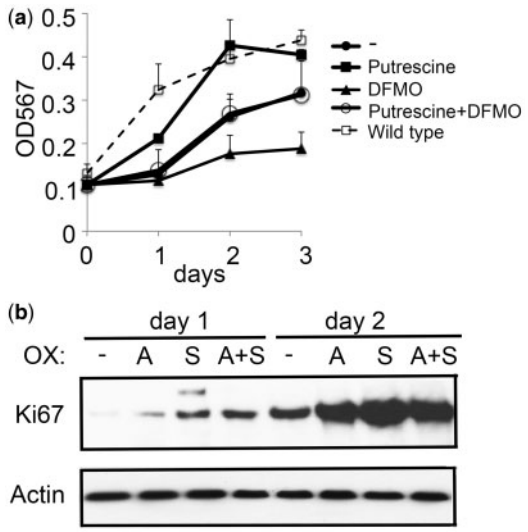

Figure 3. The effect of modulating polyamine in myoblasts. Primary myoblasts isolated from dy^{2j}/dy^{2j} EDL muscles were grown in the absence or presence of 50 μM of putrescine, 500 nM of DFMO or both (**a**). OD567 indicating formazan formation, as a measure for proliferation was taken every day and averaged. Non-stimulated wild-type myoblasts served as a control. The experiments were done in triplicates and error bars represent standard deviation. dy^{2j}/dy^{2j} myoblasts were transfected with plasmids encoding *Amd1*, *Smox* or both (**b**). Proteins were isolated after 1 and 2 days and analyzed for Ki67 and actin levels by western blot.

Lentiviral-mediated overexpression of Amd1 and Smox ameliorates dystrophic phenotypes in the dy^{2j}/dy^{2j} mice

To directly test whether the imbalance of polyamine metabolism observed between different muscle types of dy^{2j}/dy^{2j} mice plays a critical role in the disease pathogenesis of LAMA2-CMD, we generated lentiviral vectors encoding Smox or Amd1 and asked whether rescuing the expression of these genes *in vivo* could provide a therapeutic effect. Intramuscular injection in the hindlimbs of 4 days old dy^{2j}/dy^{2j} mice led to robust and sustained expression of Smox and Amd1 in the TA muscles (Fig. 4a and b). Evaluation of the protein levels showed comparable expression of Amd1 and Smox in TA and triceps in the treated groups, whereas both proteins remained lower in TA muscles of control animas treated with a GFP-encoding vector (Fig. 4a and b). Importantly, normalization of Amd1 and Smox protein levels improved muscle histopathology in TA (Fig. 4c).

We next assessed the level of classical fibrotic marker vimentin, as well as Smad2/3 phosphorylation, which indicates overactivation of profibrotic transforming growth factor (TGF)-β signaling in dystrophic muscles (7,14,15). In control GFP-injected animals, vimentin expression levels were higher in TA than triceps, supporting our observation of severe fibrosis in the hindlimb of dy^{2j}/dy^{2j} mice (Figs 2a and 4d). In contrast, the lenti-Amd1 and lenti-Smox injected TA showed reduction in the vimentin protein level to an extent similar to the triceps (Fig. 4d), and decreased level of Smad2/3 phosphorylation (Fig. 4e), which indicate attenuation of the hindlimb fibrosis as an outcome of Amd1 or Smox rescue of expression.

To assess whether there was a functional benefit of restored Amd1 and Smox expression in dy^{2j}/dy^{2j} mice, we performed open field tests at 2 months postinjection (Fig. 4f). Similar to previously reported results, the dy^{2j}/dy^{2j} mice exhibit significantly reduced mobility compared with their age- and gender-matched wild-type throughout the duration of the study (10,11), as shown by the total distance traveled of 2743.05 ± 881.23 cm and 9582.58 ± 2285.46 cm, respectively (Fig. 4f). Remarkably, the dy^{2j}/dy^{2j} mice overexpressing Amd1 and Smox were able to complete 7697.27 ± 603.93 cm and 5203.54 ± 818.01 cm distance traveled, respectively, which is significantly higher than the control animals (Fig. 4f). Collectively, these data demonstrate that restored expression of Amd and Smox improves the dystrophic phenotypes in the dy^{2j}/dy^{2j} mice, strongly implicating their capacity as protective disease modifier.

Discussion

In this study, we described presence of an imbalanced polyamine metabolism in the severely affected hindlimb TA compared with the mildly affected triceps muscles in dy^{2j}/dy^{2j} mice. Genetic rescue of Amd or Smox expression, two critical components of this pathway, significantly improved muscle fibrosis and functional motor activity of the dy^{2j}/dy^{2j} mice.

Muscle-specific phenotypic differences are commonly observed in a wide range of muscular dystrophies. For example, in limb-girdle muscular dystrophy, in which the myopathy strictly affects the limb musculature, proximal muscles are significantly more affected than distal (16). Furthermore, in dystrophin-deficient mice (*mdx*), the extraocular muscles are spared, limb muscles are moderately affected, whereas the diaphragm exhibits a very severe phenotype (17). Genome-wide expression profiling has been valuable for the discovery of novel factors involved in the dystrophic molecular signature, such as fibrosis, inflammation and failure of muscle regeneration. Previous

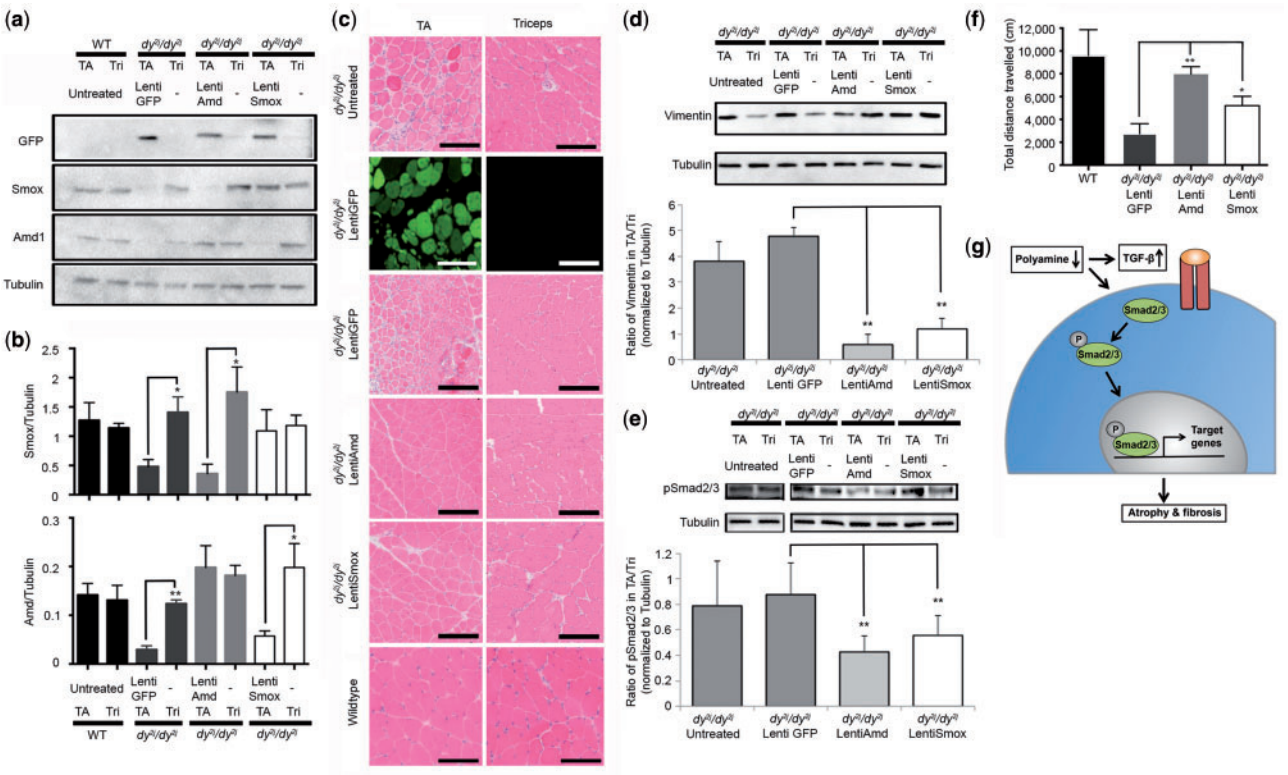

Figure 4. Overexpression of Amd1 and Smox improved dy^{2j}/dy^{2j} muscle histopathology and mobility. Hind limbs of 4-day-old dy^{2j}/dy^{2j} mice ($n = 7$ or 8/group) were injected with lentivirus carrying *GFP*, *Amd1* or *Smox* cDNAs via intramuscular injection. Sixty days postinjection, TA and triceps muscles were analyzed for the levels of GFP, Smox and Amd1 by western blot (**a**) and quantified by means of densitometry analysis (**b**). H&E staining was performed to assess muscle architecture (**c**) and the level of vimentin (**d**) and Smad2/3 phosphorylation (**e**) levels were analyzed by western blot and subsequently quantified by means of densitometry analysis. The animals were placed in open field test chamber and total distance traveled in 20 min was measured and averaged (**f**). Error bars represent the standard deviation. Statistical analysis was performed using Student's *t*-test. $^{*}P < 0.05$, $^{**}P < 0.01$. Age-matched, untreated wild-type (a, c, f) and/or dy^{2j}/dy^{2j} (c–e) mice serve as controls to clarify data presentation. Schematic overview of crosstalk between TGF-β signaling and polyamine metabolism in dystrophic muscle (**g**). Circled P indicates phosphorylation.

reports have observed reduced *Amd1* and/or *Smox* transcript levels in *mdx* (18–20) (publicly available in Gene Expression Omnibus profile database GDS2996, GDS4200) and dy^{3K}/dy^{3K} mice (21) (GDS3371), as well as muscle atrophy models in mice and rats (22,23), however, none of the studies directly interrogated the role of polyamine metabolism in the pathogenesis of muscular dystrophies. In contrast, earlier studies in human patients reported higher polyamine levels in muscle biopsies from individuals affected with myotonic dystrophy, limb-girdle muscular dystrophy and Duchenne muscular dystrophy, compared with age- and sex-matched controls (24,25). Furthermore, serum and urine polyamine levels were also elevated in these patients. However, to the best of our knowledge, there is no available data on individuals affected by MDC1A to date. In addition to the small number of patients and the type of tissues analyzed, the discrepancies between the human and mouse studies are likely attributed to differences in detection techniques, as the HPLC-MS/MS used in our and more recent studies is significantly more sensitive for metabolite analyses (22,26,27).

The cellular level of polyamines is tightly regulated through their synthesis and degradation, which is largely determined by the expression level of key enzymes in the pathway, including Amd1 and Smox. Although the regulatory control of Amd1 expression is mediated by ubiquitin-dependent proteolytic degradation at the protein level (28), it is currently not known what underlines the changes at transcriptional level. We hypothesize that transcript stability and/or rate of transcription may account for it. On the other hand, the molecular mechanism underlying posttranscriptional regulation of Smox in humans has been attributed to several miRNAs that target its 3′ Untranslated region (UTR), e.g. miR-320x and miR-139-5p (29). Further studies will be required to assess whether these mechanisms are responsible for the downregulation of Amd and Smox in dy^{2j}/dy^{2j} mice.

What is the potential mechanism of the antifibrotic property of polyamines? Depletion of polyamines in epithelial cells results in increased expression of TGF-β/TGF-β receptors, which induce phosphorylation of downstream transcription factors Smad2/3 (30). In dystrophic muscles, overactive TGF-β signaling leads to excess Smad2/3 phosphorylation and induces expression of genes responsible for impaired muscle growth and excess fibrosis (14,31–33). We propose that a decrease in polyamine levels induces excessive TGF-β signaling, and eventually exacerbates muscle atrophy and fibrosis in dy^{2j}/dy^{2j} muscles (Fig. 4g). It has also been reported that depletion of polyamines leads to mitochondria-mediated apoptosis (34), and addition of exogenous polyamines enhance satellite cell activation and expression of myogenic regulatory factors (35), providing additional mechanistic insights to be explored in the future.

Several strategies to target disease pathology in LAMA2-CMD mouse models have been explored during the past decade, aiming at compensating the loss of laminin-α2 with other extracellular matrix proteins, such as laminin-α1 (36), linker-mediated laminin-α4 (37) and mini agrin (38,39), reducing fibrosis in the muscles using losartan, an antagonist of TGF-β

signaling pathway (14) and counteracting apoptosis using Omigapil (40,41). The latter is currently in a phase I clinical trial to assess the safety profile and tolerability in patients with LAMA2- and Collagen 6-deficient CMD (clinical trial ID: NCT01805024). We have recently reported the first restoration of full-length laminin-α2 via CRISPR/Cas9-mediated correction of splicing defect in dy^{2j}/dy^{2j} mice (10). The success of this mutation-dependent approach in ameliorating disease pathophysiology, including myopathy and neuropathy, depends on efficient targeting of the CRISPR/Cas9 components to in both skeletal muscles and peripheral nerves. Restoration of laminin-α2 solely restricted to skeletal muscles was not sufficient to restore paralysis and resulted in marginal improvement of fibrosis. Future studies will assess whether synergistic therapeutic effects can be achieved when combining Lama2 restoration and polyamine modulation and focus on identification of clinically relevant genetic and/or pharmacological agents to increase polyamine levels in a variety of dystrophic animal models.

Materials and Methods

Animals

C57/BL6 and dy^{2j}/dy^{2j} animals were housed at the Johns Hopkins University School of Medicine (for the microarray experiments) and the Toronto Centre for Phenogenomics (for the remaining experiments in the study). Animal Care and Use Committee at each institution approved the experimental procedures.

RNA isolation, microarray analysis and quantitative RT-PCR

Total RNA was isolated from the indicated muscles using Trizol reagent (Invitrogen) and Qiagen RNA Clean Up (Qiagen) followed by DNase I treatment (Qiagen). Expression analysis was performed using Affymetrix 1.0 ST Gene Chip platform by Johns Hopkins Medical Institution (JHMI) High throughput Biology Center. Fold change was calculated after background substraction, normalized and then log2-transformed and used to compare expression between TA and triceps in dy^{2j}/dy^{2j} animals, and also between dy^{2j}/dy^{2j} and wild type (WT) animals.

Differentially expressed genes from these comparisons were identified after false discovery rate adjustment using Benjamini–Hochberg Step Up with *P*-value of <0.1. Top 20 downregulated and upregulated genes have ≥ 3.27- and 2.66-fold change, respectively. cDNA was synthesized from 500 ng of total RNA using oligo d(T) primers and SuperScript III kit (ThermoFisher) according to manufacturer's protocol. Quantitative qRT-PCR was performed using TaqMan probes for *Smox* and *Amd1* normalized to 18s RNA.

Histology and western blotting

Muscles were flash-frozen in cooled isopentane, mounted in Tissue-Tek (Sakura), sectioned at 8 μm thickness and stained with hematoxylin–eosin (H&E). Intervening regions of the muscle sections were collected in 1.4 mm Zirconium Beads prefilled tubes (OPS Diagnostics) for proteins isolation. Sectioned muscles were lysed in 500 μl of RIPA homogenizer buffer [50 mM Tris–HCl pH 7.4, 150 nM NaCl, 1 mM EDTA supplemented with Phosphatase and Protease inhibitor cocktails (Roche)] using MagNA Lyser (Roche). Following three to four steps of homogenization at 10 s each, 500 μl of RIPA double detergents buffer (2% deoxycholate, 2% NP40 and 2% Triton X-100 in RIPA homogenizer buffer) was added to the lysates, which were then incubated for 45 min at 4°C with rotation and centrifuged for 10 min at 30 000*g*. The protein concentration of the supernatant was measured using the BCA assay (Thermo Fisher). Six micrograms of proteins were run on NuPAGE 4–12% Bis-Tris protein gels and transferred using the Novex systems (Life Technologies) according to manufacturer's protocol.

The primary antibodies used in this studies were mouse monoclonal anti-Amd (SC-166970; 1:250), β-actin (SC-47778; 1:5000), rabbit polyclonal anti-Ki67 (AB15580; 1:500), Vimentin (Developmental Studies Hybridoma Bank, DSHB; 1:2500), Smox (SAB1101510; 1:250), phospho-Smad2/Smad3 (Cell signaling, mAB-8828s, 1:1000), GFP (AB-32146; 1:1000) and tubulin (1:5000). The signal was detected using Femto enhanced chemiluminescent (Thermo Fisher) in a Bio-Rad ChemiDoc Imaging and densitometry analysis was performed using Image J software.

High performance liquid chromatography/mass spectrometry (HPLC-MS/MS)

Quantification of muscle polyamine level was performed at the Analytical Facility for Bioactive Molecule at SickKids based on the method described by Byun *et al.* (42) with slight modification. Muscles were homogenized in PBS to a concentration of 5 mg/ml. Protein concentration was measured by BCA assay. The samples underwent a protein crush in methanol, were brought to a pH of 9.0 with 1M sodium carbonate and then carbamoylated with isobutyl chloroformate at 37°C and further extracted with diethyl ether twice. Samples were dried under N2 and reconstituted in 1:1 H_2O: acetonitrile + 0.2% acetic acid prior to analysis by LC/MS/MS (API 4000 with Agilent 1200 HPLC, on an Agilent Eclipse XDB-C18 150 × 4.6 mm, 5 μm column). The concentration of each polyamine was interpolated to the standard curve from commercially available polyamine standards (Sigma-Aldrich) and expressed as ng/mg of protein.

Cell culture

Primary myoblasts were isolated from extensor digitorum longus (EDL) of 3-week-old WT or dy^{2j}/dy^{2j} mice using previously described method (43). Proliferation assay was performed using CellTiter 96 non-radioactive cell proliferation assay (Promega). Eflornithine hydrochloride (DFMO; ApiChemistry) and putrescine (Sigma-Aldrich) were supplemented into the cells at a concentration of 500 nM and 50 μM, respectively.

Lentiviral production, titer quantification and injection

Amd and *Smox* cDNA were purchased from Origene and cloned into CEP transfer plasmid using Gibson Assembly (New England Biolabs). Lentivirus were produced by cotransfecting 5 μg of transfer plasmid, 6.5 μg of REV responsive element (RRE), 3.5 μg of VSVG envelope and 2.5 μg of REV into HEK293T cells using Calcium phosphate method. Supernatant was collected 4 and 5 days posttransfection and filtered through 0.45 μm low-binding filter (EMD Millipore), centrifuged at 50 000*g* for 140 min at 4C. Viral supernatant was aliquoted and stored at −80°C prior to use. Titer was determined via flow cytometry. In brief, 293T cells were plated at 2.10^5 cells/well in a 12-wells plate. On day 2, cell number was determined and cells were transduced with 5–500 μl of crude supernatant in total of 500 μl of DMEM and 10% FBS. Three days later, the cells were trypsinized, centrifuged at 500*g* for 5 min and fixed with 1% formaldehyde in PBS for 5 min. The

cells were washed once before resuspended in 1X PBS. Titer was calculated as {F × (Co/V)} × D, in which F is the number of GFP+ cells, Co is number of cell at day 2, V is the volume of virus and D is dilution factor. Lentiviral titer obtained is around 2×10^{10} transduction unit (TU)/ml. For *in vivo* experiment, 10^8 TU/limb was injected into each hindlimb of 4-day-old mice and muscles were isolated at the indicated time points.

Open field activity

Mice are transported to the experimental room 30 minutes prior to the test. Each open field arena (43.5 cm^2 with three 16 beam IR arrays, illuminated with 275 lux LED lights) is divided into a peripheral zone measuring 8 cm from the edge of the arena walls, and a central zone around 40% of the total surface of the arena. Testing is conducted during light phase of the cycle with 1 hour gap from the light/dark change. Each mouse is placed in the middle of a peripheral zone of the arena facing the wall and allowed to explore the apparatus freely for 20 minutes. Total distance travelled was recorded using VersaMax Animal Activity Monitoring System.

Supplementary Material

Supplementary Material is available at *HMG* online.

Conflict of Interest statement. None declared.

Funding

This work was supported by Association Francaise contre les Myopathies (AFM)-Telethon postdoctoral fellowship number 18253, Cure CMD (to D.U.K); Natural Sciences and Engineering Research Council of Canada RGPIN-2014-04143, SickKids Foundation and R.S. McLaughlin Foundation Chair in Pediatrics (to R.D.C).

Acknowledgements

The authors thank Drs Jayne Danska, Tanya Prasolava and Andrei Malko at the Hospital for Sick Children, Toronto for providing us with the lentiviral vectors used in this study, Hayley Craig-Barnes and Michael Leadley at the Analytical Facility for Bioactive Molecules of the Centre for the Study of Complex Childhood Diseases for assistance with polyamine quantification, Igor Vukobradovic at the Lunenfeld-Tanenbaum Research Institute's Centre for Modeling Human Disease Mouse Phenotyping Facility for performing the open field tests and The Toronto Centre for Phenogenomics staff for mouse husbandry and colony maintenance. They also thank the Cohn Lab members for excellent technical assistance and critical input to the article.

References

1. Gawlik, K.I. and Durbeej, M. (2011) Skeletal muscle laminin and MDC1A: pathogenesis and treatment strategies. *Skelet. Muscle*, **1**, 9.
2. Desaki, J., Matsuda, S. and Sakanaka, M. (1995) Morphological changes of neuromuscular junctions in the dystrophic (dy) mouse: a scanning and transmission electron microscopic study. *J. Electron Microsc.*, **44**, 59–65.
3. Homma, S., Beermann, M.L. and Miller, J.B. (2011) Peripheral nerve pathology, including aberrant Schwann cell differentiation, is ameliorated by doxycycline in a laminin-alpha2-deficient mouse model of congenital muscular dystrophy. *Hum. Mol. Genet.*, **20**, 2662–2672.
4. Bonnemann, C.G., Wang, C.H., Quijano-Roy, S., Deconinck, N., Bertini, E., Ferreiro, A., Muntoni, F., Sewry, C., Beroud, C., Mathews, K.D. *et al.* (2014) Diagnostic approach to the congenital muscular dystrophies. *Neuromuscul. Disord.*, **24**, 289–311.
5. Allamand, V. and Guicheney, P. (2002) Merosin-deficient congenital muscular dystrophy, autosomal recessive (MDC1A, MIM#156225, LAMA2 gene coding for alpha2 chain of laminin). *Eur. J. Hum. Genet.*, **10**, 91–94.
6. Geranmayeh, F., Clement, E., Feng, L.H., Sewry, C., Pagan, J., Mein, R., Abbs, S., Brueton, L., Childs, A.M., Jungbluth, H. *et al.* (2010) Genotype-phenotype correlation in a large population of muscular dystrophy patients with LAMA2 mutations. *Neuromuscul. Disord.*, **20**, 241–250.
7. Mehuron, T., Kumar, A., Duarte, L., Yamauchi, J., Accorsi, A. and Girgenrath, M. (2014) Dysregulation of matricellular proteins is an early signature of pathology in laminin-deficient muscular dystrophy. *Skelet. Muscle*, **4**, 14.
8. Xu, H., Wu, X.R., Wewer, U.M. and Engvall, E. (1994) Murine muscular dystrophy caused by a mutation in the laminin alpha 2 (Lama2) gene. *Nat. Genet.*, **8**, 297–302.
9. Sunada, Y., Bernier, S.M., Utani, A., Yamada, Y. and Campbell, K.P. (1995) Identification of a novel mutant transcript of laminin alpha 2 chain gene responsible for muscular dystrophy and dysmyelination in dy2J mice. *Hum. Mol. Genet.*, **4**, 1055–1061.
10. Kemaladewi, D.U., Maino, E., Hyatt, E., Hou, H., Ding, M., Place, K.M., Zhu, X., Bassi, P., Baghestani, Z., Deshwar, A.G. *et al.* (2017) Correction of a splicing defect in a mouse model of congenital muscular dystrophy type 1A using a homology-directed-repair-independent mechanism. *Nat. Med.*, **23**, 984–989.
11. Tatem, K.S., Quinn, J.L., Phadke, A., Yu, Q., Gordish-Dressman, H. and Nagaraju, K. (2014) Behavioral and locomotor measurements using an open field activity monitoring system for skeletal muscle diseases. *J. Vis. Exp.*, **91**, 51785.
12. Mandal, S., Mandal, A., Johansson, H.E., Orjalo, A.V. and Park, M.H. (2013) Depletion of cellular polyamines, spermidine and spermine, causes a total arrest in translation and growth in mammalian cells. *Proc. Natl. Acad. Sci. U. S. A.*, **110**, 2169–2174.
13. Casero, R.A., Jr and Marton, L.J. (2007) Targeting polyamine metabolism and function in cancer and other hyperproliferative diseases. *Nat. Rev. Drug Discov.*, **6**, 373–390.
14. Elbaz, M., Yanay, N., Aga-Mizrachi, S., Brunschwig, Z., Kassis, I., Ettinger, K., Barak, V. and Nevo, Y. (2012) Losartan, a therapeutic candidate in congenital muscular dystrophy: studies in the dy(2J)/dy(2J) mouse. *Ann. Neurol.*, **71**, 699–708.
15. Goldstein, J.A., Bogdanovich, S., Beiriger, A., Wren, L.M., Rossi, A.E., Gao, Q.Q., Gardner, B.B., Earley, J.U., Molkentin, J.D. and McNally, E.M. (2014) Excess SMAD signaling contributes to heart and muscle dysfunction in muscular dystrophy. *Hum. Mol. Genet.*, **23**, 6722–6731.
16. Semplicini, C., Vissing, J., Dahlqvist, J.R., Stojkovic, T., Bello, L., Witting, N., Duno, M., Leturcq, F., Bertolin, C., D'Ambrosio, P. *et al.* (2015) Clinical and genetic spectrum in limb-girdle muscular dystrophy type 2E. *Neurology*, **84**, 1772–1781.
17. Stedman, H.H., Sweeney, H.L., Shrager, J.B., Maguire, H.C., Panettieri, R.A., Petrof, B., Narusawa, M., Leferovich, J.M., Sladky, J.T. and Kelly, A.M. (1991) The mdx mouse

diaphragm reproduces the degenerative changes of Duchenne muscular dystrophy. *Nature*, **352**, 536–539.
18. Porter, J.D., Merriam, A.P., Leahy, P., Gong, B. and Khanna, S. (2003) Dissection of temporal gene expression signatures of affected and spared muscle groups in dystrophin-deficient (mdx) mice. *Hum. Mol. Genet.*, **12**, 1813–1821.
19. Reynolds, J.G., McCalmon, S.A., Donaghey, J.A. and Naya, F.J. (2008) Deregulated protein kinase A signaling and myospryn expression in muscular dystrophy. *J. Biol. Chem.*, **283**, 8070–8074.
20. Chandrasekharan, K., Yoon, J.H., Xu, Y., deVries, S., Camboni, M., Janssen, P.M., Varki, A. and Martin, P.T. (2010) A human-specific deletion in mouse Cmah increases disease severity in the mdx model of Duchenne muscular dystrophy. *Sci. Transl. Med.*, **2**, 42ra54.
21. Hager, M., Bigotti, M.G., Meszaros, R., Carmignac, V., Holmberg, J., Allamand, V., Akerlund, M., Kalamajski, S., Brancaccio, A., Mayer, U. *et al.* (2008) Cib2 binds integrin alpha7Bbeta1D and is reduced in laminin alpha2 chain-deficient muscular dystrophy. *J. Biol. Chem.*, **283**, 24760–24769.
22. Bongers, K.S., Fox, D.K., Kunkel, S.D., Stebounova, L.V., Murry, D.J., Pufall, M.A., Ebert, S.M., Dyle, M.C., Bullard, S.A., Dierdorff, J.M. *et al.* (2015) Spermine oxidase maintains basal skeletal muscle gene expression and fiber size and is strongly repressed by conditions that cause skeletal muscle atrophy. *Am. J. Physiol. Endocrinol. Metab.*, **308**, E144–E158.
23. Lorenzini, E.C., Colombo, B., Ferioli, M.E., Scalabrino, G. and Canal, N. (1989) Polyamine biosynthetic decarboxylases in muscles of rats with different experimental myopathies. *J. Neurol. Sci.*, **89**, 27–35.
24. Rudman, D., Kutner, M.H., Chawla, R.K. and Goldsmith, M.A. (1980) Abnormal polyamine metabolism in hereditary muscular dystrophies: effect of human growth hormone. *J. Clin. Invest.*, **65**, 95–102.
25. Kaminska, A., Stern, L. and Russel, D. (1981) Polyamine accumulation in normal and denervated neonatal muscle. *Exp. Neurol.*, **72**, 612–818.
26. Magnes, C., Fauland, A., Gander, E., Narath, S., Ratzer, M., Eisenberg, T., Madeo, F., Pieber, T. and Sinner, F. (2014) Polyamines in biological samples: rapid and robust quantification by solid-phase extraction online-coupled to liquid chromatography-tandem mass spectrometry. *J. Chromatogr. A*, **1331**, 44–51.
27. Hinderer, C., Katz, N., Louboutin, J.-P., Bell, P., Tolar, J., Orchard, P.J., Lund, T.C., Nayal, M., Weng, L., Mesaros, C. *et al.* (2017) Abnormal polyamine metabolism is unique to the neuropathic forms of MPS: potential for biomarker development and insight into pathogenesis. *Hum. Mol. Genet.*, **26**, 3837–3849.
28. Yerlikaya, A. and Stanley, B.A. (2004) S-adenosylmethionine decarboxylase degradation by the 26 S proteasome is accelerated by substrate-mediated transamination. *J. Biol. Chem.*, **279**, 12469–12478.
29. Lopez, J.P., Fiori, L.M., Gross, J.A., Labonte, B., Yerko, V., Mechawar, N. and Turecki, G. (2014) Regulatory role of miRNAs in polyamine gene expression in the prefrontal cortex of depressed suicide completers. *Int. J. Neuropsychopharmacol.*, **17**, 23–32.
30. Liu, L., Santora, R., Rao, J.N., Guo, X., Zou, T., Zhang, H.M., Turner, D.J. and Wang, J.Y. (2003) Activation of TGF-beta-Smad signaling pathway following polyamine depletion in intestinal epithelial cells. *Am. J. Physiol. Gastrointest. Liver Physiol.*, **285**, G1056–G1067.
31. Kemaladewi, D.U., 't Hoen, P.A.C., ten Dijke, P., van Ommen, G.J.B. and Hoogaars, W.M. (2012) TGF-β signaling in Duchenne muscular dystrophy. *Future Neurol.*, **7**, 209–224.
32. Cohn, R.D., van Erp, C., Habashi, J.P., Soleimani, A.A., Klein, E.C., Lisi, M.T., Gamradt, M., ap Rhys, C.M., Holm, T.M., Loeys, B.L. *et al.* (2007) Angiotensin II type 1 receptor blockade attenuates TGF-beta-induced failure of muscle regeneration in multiple myopathic states. *Nat. Med.*, **13**, 204–210.
33. Burks, T.N. and Cohn, R.D. (2011) Role of TGF-beta signaling in inherited and acquired myopathies. *Skelet. Muscle*, **1**, 19.
34. Mandal, S., Mandal, A. and Park, M.H. (2015) Depletion of the polyamines spermidine and spermine by overexpression of spermidine/spermine N(1)-acetyltransferase 1 (SAT1) leads to mitochondria-mediated apoptosis in mammalian cells. *Biochem. J.*, **468**, 435–447.
35. Thornton, K.J., Chapalamadugu, K.C., Doumit, M.E. and Murdoch, G.K. (2013) Polyamines enhance satellite cell activation and expression of myogenic regulatory factors. *FASEB J.*, **27**, 1146–1147.
36. Rooney, J.E., Gurpur, P.B. and Burkin, D.J. (2009) Laminin-111 protein therapy prevents muscle disease in the mdx mouse model for Duchenne muscular dystrophy. *Proc. Natl. Acad. Sci. U. S. A.*, **106**, 7991–7996.
37. Reinhard, J.R., Lin, S., McKee, K.K., Meinen, S., Crosson, S.C., Sury, M., Hobbs, S., Maier, G., Yurchenco, P.D. and Ruegg, M.A. (2017) Linker proteins restore basement membrane and correct LAMA2-related muscular dystrophy in mice. *Sci. Transl. Med.*, **9**, 396.
38. Qiao, C., Li, J., Zhu, T., Draviam, R., Watkins, S., Ye, X., Chen, C., Li, J. and Xiao, X. (2005) Amelioration of laminin-alpha2-deficient congenital muscular dystrophy by somatic gene transfer of miniagrin. *Proc. Natl. Acad. Sci. U. S. A.*, **102**, 11999–12004.
39. Meinen, S., Lin, S., Thurnherr, R., Erb, M., Meier, T. and Ruegg, M.A. (2011) Apoptosis inhibitors and mini-agrin have additive benefits in congenital muscular dystrophy mice. *EMBO Mol. Med.*, **3**, 465–479.
40. Erb, M., Meinen, S., Barzaghi, P., Sumanovski, L.T., Courdier-Fruh, I., Ruegg, M.A. and Meier, T. (2009) Omigapil ameliorates the pathology of muscle dystrophy caused by laminin-alpha2 deficiency. *J. Pharmacol. Exp. Therap.*, **331**, 787–795.
41. Yu, Q., Sali, A., Van der Meulen, J., Creeden, B.K., Gordish-Dressman, H., Rutkowski, A., Rayavarapu, S., Uaesoontrachoon, K., Huynh, T., Nagaraju, K. *et al.* (2013) Omigapil treatment decreases fibrosis and improves respiratory rate in dy(2J) mouse model of congenital muscular dystrophy. *PLoS One*, **8**, e65468.
42. Byun, J.A., Lee, S.H., Jung, B.H., Choi, M.H., Moon, M.H. and Chung, B.C. (2008) Analysis of polyamines as carbamoyl derivatives in urine and serum by liquid chromatography-tandem mass spectrometry. *Biomed. Chromatogr.*, **22**, 73–80.
43. Collins, C.A. and Zammit, P.S. (2009) Isolation and grafting of single muscle fibres. *Methods Mol. Biol.*, **482**, 319–330.